

Vesicular ATP release from hepatocytes plays a role in the progression of nonalcoholic steatohepatitis

辰島, 啓太

<https://hdl.handle.net/2324/6758960>

出版情報 : Kyushu University, 2022, 博士 (医学), 論文博士
バージョン :
権利関係 : (c) 2020 Elsevier B.V. All rights reserved.





Contents lists available at ScienceDirect

BBA - Molecular Basis of Disease

journal homepage: www.elsevier.com/locate/bbadis

Vesicular ATP release from hepatocytes plays a role in the progression of nonalcoholic steatohepatitis

Keita Tatsushima^{a,b,c}, Nao Hasuzawa^{a,d}, Lixiang Wang^e, Miki Hiasa^f, Shohei Sakamoto^a, Kenji Ashida^{a,d}, Nobuyuki Sudo^b, Yoshinori Moriyama^{d,f,*}, Masatoshi Nomura^{a,d,*}

^a Department of Medicine and Bioregulatory Science, Graduate School of Medical Sciences, Kyushu University, Fukuoka 812-8582, Japan

^b Department of Psychosomatic Medicine, Graduate School of Medical Sciences, Kyushu University, Fukuoka 812-8582, Japan

^c Endocrine Center, Toranomon Hospital, Tokyo 105-8470, Japan

^d Division of Endocrinology and Metabolism, Department of Internal Medicine, Kurume University School of Medicine, Kurume 830-0011, Japan

^e Department of Medical Biochemistry, Kurume University School of Medicine, Kurume 830-0011, Japan

^f Department of Membrane Biochemistry, Graduate School of Medicine, Dentistry and Pharmaceutical Sciences, Okayama University, Okayama 700-8530, Japan

ARTICLE INFO

Keywords:

ATP
Inflammation
NASH
Triglyceride
VNUT
Hepatocyte
VLDL
Apolipoprotein B
SLC17A9
Purinergic signaling

ABSTRACT

Non-alcoholic steatohepatitis (NASH) is becoming a growing public health problem along with the increase of metabolic syndrome worldwide. Extracellular nucleotides are known to serve as a danger signal by initiating purinergic signaling in many inflammatory disorders, although the role of purinergic signaling in the progression of NASH remains to be clarified. Vesicular nucleotide transporter (VNUT) is a key molecule responsible for vesicular ATP release to initiate purinergic signaling. Here, we studied the role of VNUT in the progression of nonalcoholic steatohepatitis. VNUT was expressed in mouse hepatocytes and associated, at least in part, with apolipoprotein B (apoB)-containing vesicles. High glucose stimulation evoked release of appreciable amount of ATP from hepatocytes, which disappeared in hepatocytes of *Vnut* knockout (*Vnut*^{−/−}) mice. Glucose treatment also stimulated triglyceride secretion from hepatocytes, which was inhibited by PPADS and MRS211, antagonists of P2Y receptors, and clodronate, a VNUT inhibitor, and was significantly reduced in *Vnut*^{−/−} mice. *In vivo*, postprandial secretion of triglyceride from hepatocytes was observed, while the serum triglyceride level was significantly reduced in *Vnut*^{−/−} mice. On a high-fat diet, the liver of wild type mice exhibited severe inflammation, fibrosis, and macrophage infiltration, which is similar to NASH in humans, while this NASH pathology was not observed in *Vnut*^{−/−} mice. These results suggest that VNUT-mediated vesicular ATP release regulates triglyceride secretion and involves in chronic inflammation in hepatocytes. Since blockade of vesicular ATP release protects against progression of steatohepatitis, VNUT may be a pharmacological target for NASH.

Abbreviations: Acc, acetyl-CoA carboxylase; ALT, alanine aminotransferase; ApoA4/5, apolipoprotein A-IV/V; ApoB, apolipoprotein B; AST, aspartate aminotransferase; Col1a1, collagen type1 alpha1; Cpt1a, carnitine palmitoyltransferase 1a; EEA1, early endosome antigen 1; Elovl3, elongation of very long chain-fatty acids; Fasn, fatty acid synthase; Fgf21, fibroblast growth factor 21; GAPDH, glyceraldehyde 3-phosphate dehydrogenase; HFD, high fat diet; Insig1, Insulin Induced Gene 1; LAMP1, lysosomal associated membrane protein 1; LPL, lipoprotein lipase; Mcp-1, monocyte chemotactic protein-1; MRS2211, 2-[(2-chloro-5-nitrophenyl)azo]-5-hydroxy-6-methyl-3-[(phosphonoxy)methyl]-4-pyridinecarboxaldehyde disodium salt; Mttp, microsomal triglyceride transfer protein; NAFLD, nonalcoholic fatty liver disease; NASH, non-alcoholic steatohepatitis; NCD, normal chow diet; NEFA, non-esterified fatty acid; PDI, anti-protein disulfide isomerase; P2Y receptor, purinergic 2Y receptor; PPADS, pyridoxalphosphate-6-azophenyl-2', 4'-disulfonic acid; Ppara, peroxisome proliferator-activated receptor alpha; Scd1, stearoyl-CoA desaturase-1; SLC17A9, solute carrier family 17 member 9; Srebf1, sterol regulatory element-binding transcription factor 1; Srebp1, sterol regulatory element-binding protein; Tgfb, transforming growth factor beta; HSCs, hepatic stellate cells; Tie2, tyrosine kinase with Ig-like loops and epidermal growth factor homology domains-2; Timp1, tissue inhibitor of metalloproteinase; VAMP7, vesicle-associated membrane protein 7; VNUT, vesicular nucleotide transporter.

* Corresponding authors at: Division of Endocrinology and Metabolism, Department of Internal Medicine, Kurume University School of Medicine, 67 Asahi-machi, Kurume 830-0011, Japan.

E-mail addresses: moriyama.yoshinori@med.kurume-u.ac.jp (Y. Moriyama), nomura@med.kurume-u.ac.jp (M. Nomura).

<https://doi.org/10.1016/j.bbadis.2020.166013>

Received 17 June 2020; Received in revised form 3 November 2020; Accepted 9 November 2020

Available online 17 November 2020

0925-4439/© 2020 Elsevier B.V. All rights reserved.

1. Introduction

Nonalcoholic fatty liver disease (NAFLD) is now considered to be the most common cause of chronic liver disease worldwide and affects 20%–40% of the general population [1]. NAFLD comprises simple steatosis and nonalcoholic steatohepatitis (NASH); the latter is characterized by hepatocyte injury, liver inflammation, and progression of fibrosis, and it can progress to liver cirrhosis, liver failure, and hepatocellular carcinoma. NAFLD is often associated with components of metabolic syndrome such as abdominal obesity, insulin resistance, hypertension, and dyslipidemia. Thus, metabolic syndrome is a main risk factor for NAFLD. Because portal blood flow leads to the exposure of non-esterified fatty acid (NEFA) and pro-inflammatory cytokines in liver tissues, accumulation of visceral adipose tissues directly influences the NAFLD development by affecting NEFA influx, *de novo* lipid synthesis, oxidative stress, and inflammation in the liver. Additionally, the accumulation of visceral fat also involves chronic inflammation, which leads to atherosclerotic disorders such as ischemic heart disease and cerebral infarction [2]. Although the strong correlation between NAFLD and metabolic syndrome has been studied, their causative association with NASH is not fully understood.

Purinergic signaling is one of the major regulatory systems in the liver functions such as bile secretion and glycogenesis, and its changes affect components of metabolic syndrome such as inflammation and insulin resistance [3–9]. Hepatocytes secrete ATP into different extracellular spaces *via* basolateral, sinusoidal or apical membranes [4]. The extracellular ATP then undergoes successive hydrolysis in the extracellular space by Cd39, ecto-ATPase, and the resultant products, ADP and adenosine, in addition to ATP, bind to their respective purinergic receptors on liver cells in an autocrine and/or paracrine manner [3–9]. Cd39 has been shown to induce endocytosis of high-density lipoproteins (HDL) and stimulate very low-density lipoprotein (VLDL) secretion in the liver [10,11]. Mice lacking Cd39 showed hepatic insulin resistance and increased serum triglyceride levels, possibly due to elevated ATP concentrations by impaired extracellular nucleotide degradation [10]. Cd39 polymorphisms are associated with type 2 diabetes and diabetic nephropathy [11]. Moreover, in human peripheral monocytes, the expression of Cd39 is higher in type 2 diabetes patients compared with normal subjects, suggesting a compensation mechanism against the inflammation generated by P2X7 receptors during macrophages responses [12]. Thus, purinergic signaling involves regulation of glucose and lipid metabolisms in the liver. Type 2 diabetes and NASH may also be associated with chronic nucleotide secretion leading to an activation of purinergic signaling [13].

Vesicular nucleotide transporter (VNUT) belongs to solute carrier family 17 member 9 (SLC17A9) and is responsible for vesicular storage of ATP in various ATP-secreting cells [14–16]. Mice lacking VNUT lost vesicular storage and secretion of ATP in almost all ATP-secreting cells tested so far, thus, being regarded as an essential membrane component to initiate purinergic signaling [15,16]. Previously we observed that VNUT-dependent ATP release and activation of purinergic signaling aggravates glucose metabolism by reducing insulin sensitivity in the liver [15,16], providing direct evidence that purinergic signaling is involved in glucose homeostasis. We wonder if VNUT is responsible for vesicular ATP release in hepatocytes and, if so, VNUT-induced purinergic signaling could play a role in hepatic lipid metabolism and in NASH development.

In the present study, we show that VNUT is expressed in hepatocyte, and VNUT-dependent vesicular ATP release triggers postprandial triglyceride release and aggravates steatohepatitis through P2Y receptor signaling in the liver.

2. Materials and methods

2.1. Animal experiments

All mouse procedures and protocols were conducted in accordance with the Guide for the Care and Use of Laboratory Animals and were approved by the Ethics Committees on Animal Experimentation from Kyushu University, Kurume University and Okayama University. Vesicular nucleotide transporter deficient (*Vnut*^{−/−}) mice on a C57BL/6 J background were generated as described [15]. Mice were maintained in a temperature-controlled, specific pathogen-free environment (12 h light–12 h dark cycle; room temperature, 22–24 °C; 50–60% relative humidity). Mice were fed a normal chow diet (NCD) or high fat diet (HFD) (45 kcal % fat, D12451; Research Diets Inc., New Brunswick, NJ, USA) *ad libitum* and weighed weekly. Food intake was measured every 4 min for 3 days from individually housed mice using a food consumption monitor system (NeuroScience Idea Co. Ltd., Osaka, Japan). There was no statistical difference in body weight and organ weights (liver and gonadal adipose tissue) between WT and *Vnut*^{−/−} mice fed either NCD for 28 weeks or HFD for 48 weeks (Electronic Supplementary Material (ESM) Fig. 1). Food intake was not altered between the genotypes at any points analyzed.

Blood samples were taken from the tail vein of 8-week-old mice after an 18-h fast and then mice were refed for 4 h. Serum triglyceride, total cholesterol, and NEFA concentrations were determined using assay kits (Wako Pure Chemical Industries Ltd., Saitama, Japan). Plasma glucose concentration was measured using Glutest Every (Sanwa Kagaku Kenkyusho Co. Ltd., Aichi, Japan). Alanine aminotransferase (ALT) and aspartate aminotransferase (AST) were measured using a Fuji drychem slide, as follows: GOT/AST-PIII, GPT/ALT-PIII (Fujifilm Corporation, Tokyo, Japan). Hepatic lipids were extracted from murine livers using Folch's method [17]. To extract hepatic ATP, we used the phenol–TE extraction method, as previously described [18]. The ATP concentration was measured using a luciferin–luciferase assay kit (Kinsiro, Toyo B-Net Co., Ltd., Tokyo, Japan). To measure the VLDL secretion rate *in vivo*, mice were injected with tyloxapol (Triton-1339, Sigma-Aldrich, Inc. St. Louis, MO, USA) (500 mg/kg in saline) intraperitoneally after an 18-h fast. Blood samples were collected at 0, 1, 2, and 4 h thereafter, as previously described [19].

2.2. Primary culture of mouse hepatocytes

See Electronic Supplementary Material (ESM) Methods for details.

2.3. *In vitro* measurement of ATP and triglyceride secretion

ATP release was assayed as described [7]. See ESM Methods for details. To inhibit or activate purinergic signaling, primary cultured hepatocytes were pretreated with each of following compounds: 100 μM of Suramin (P2X receptor antagonist), 100 μM of pyridoxalphosphate-6-azophenyl-2',4'-disulfonic acid (PPADS, P2Y receptor antagonist), 100 μM of 2-[(2-chloro-5-nitrophenyl)azo]-5-hydroxy-6-methyl-3-[(phosphonoxy)methyl]-4-pyridinecarboxaldehyde disodium salt (MRS2211, P2Y13 receptor antagonist), 100 μM of 2-methylthioadenosine diphosphate trisodium salt (2-methylthio-ADP) [20], or 100 μM of clodronate (VNUT inhibitor [21,22]) for 20 min. Subsequently, the cells were stimulated by 25 mM of glucose for 60 min, and the ATP and triglyceride levels were measured in the medium. Suramin, PPADS, MRS2211, and 2-methylthio-ADP were from TOCRIS bioscience (Bristol, UK), and clodronate was from Sigma-Aldrich (St. Louis, MO, USA). Hepatocytes were seeded at 2×10^5 cells/well on 12-well plastic plates. All experiments were performed at least three times. Each independent experiment was run in triplicate or duplicate plates and these were used to generate a single mean value, which was then used to generate the mean ± standard error of the mean (SEM) shown in the figure.

2.4. Immunohistochemistry

For indirect immunofluorescence microscopy, published procedures were used [14,15]. In brief, hepatocytes on collagen type I and poly-L-lysine-coated coverslips were fixed with 4% paraformaldehyde in phosphate-buffered saline (PBS) for 30 min at room temperature. The cells were washed with PBS and incubated with the same buffer containing 0.1% Triton X-100 for 20 min, and then further incubated with 2% goat serum and 0.5% BSA in the same buffer for 30 min at room temperature. Primary antibody treatment was performed using antibodies specific for VNUT (1:100), ApoB (1:200), LAMP1 (1:100), EEA1 (1:100), and PDI (1:100) in PBS containing 0.5% BSA for 1 h at room temperature. The secondary antibodies used were Alexa Fluor 488-labeled anti-rabbit IgG (1:500) and Alexa Fluor 568-labeled anti-mouse IgG (1:1000) (Molecular Probes, Eugene, OR, USA) or Alexa Fluor 594-labeled anti-chicken IgY (1:1000) (Abcam). The specimens were observed using an Olympus FV300 confocal laser microscope. The specificity of rabbit polyclonal antibodies against human and mouse VNUT prepared in-house were determined as described previously [14,15]. Quantitative analysis of colocalization with M1 and M2 coefficients using the JACoP plugin in ImageJ. The following antibodies were obtained commercially: anti-VAMP7 mouse monoclonal (Abcam), anti-LAMP1 mouse monoclonal (StressMarq Biosciences, Victoria, BC, Canada), anti-EEA1 mouse monoclonal (BD Biosciences), anti-PDI mouse monoclonal (Abcam), and anti-ApoB chicken polyclonal antibodies (Abcam).

2.5. Histological analyses

See EMS Methods for details. Histological evaluation of NAFLD was performed in accordance with the scoring system that was proposed by the Nonalcoholic Steatohepatitis Clinical Research Network [23]. Histological features were evaluated semi-quantitatively, as follows: steatosis (0–3), lobular inflammation (0–2), and hepatocellular ballooning (0–2).

2.6. Total RNA isolation, real time-PCR, and microarray procedures

Total RNA was isolated using TRIzol (Invitrogen Corporation, Carlsbad, CA, USA) from liver and primary cultured hepatocytes. RNA samples were quantified by an ND-1000 spectrophotometer (NanoDrop Technologies, Wilmington, DE, USA), and reverse transcribed to cDNA using the QuantiTect Reverse Transcription Kit (Qiagen, Hilden, Germany). Quantitative real-time RT-PCR was performed using SYBR(R) Premix ExTaq TMII (Takara-Bio Inc., Shiga, Japan) in Applied Biosystems 7500 (Bio-Rad Laboratories, Inc., Hercules, CA, USA) as a described menu. We used glyceraldehyde 3-phosphate dehydrogenase (GAPDH) to normalize the results. PCR was performed using Go Taq (R) Green Master Mix (Promega KK) in a C1000 touch TM thermal cycler (Bio-Rad Laboratories, Inc.) with specific primer sets (ESM Table 1). For the microarray assay, the cRNA was amplified, labeled, and hybridized to a 44 K Agilent 60-mer oligomicroarray, in accordance with the manufacturer's instructions (Agilent Technologies, Inc., Santa Clara, CA, USA). An Agilent scanner scanned all hybridized microarray slides. Relative hybridization intensities and background hybridization values were calculated using Agilent Feature Extraction Software (9.5.1.1). See ESM Methods for details of the data analysis and filter criteria.

2.7. Statistics analysis

Data are expressed as the mean \pm standard error of the mean (SEM). Statistical evaluation of differences between the experimental groups was determined using the Welch's *t*-test or one-way analysis of variance (ANOVA) with Dunnett's multiple comparison tests. For the feeding test and tyloxapol injection test, a two-way repeated measure ANOVA was used. All analyses were performed using JMP version 11.0 (SAS Institute

Japan Inc., Tokyo, Japan). The significant difference value was set as $P < 0.05$.

3. Results

3.1. VNUT is expressed in hepatocytes

Two major cell types, hepatocytes and mesenchymal cells, populate the liver lobes. Although we have previously shown that the *Vnut* gene is expressed in the mouse liver [14,15], whether hepatocytes express *Vnut* remains undetermined. As the first step of the study, we analyzed whether or not hepatocytes express VNUT. As shown in Fig. 1a, RT-PCR analysis of mRNA of whole liver and the isolated hepatocytes, *Vnut* expression was found in the isolated hepatocyte. Little *Tie2* and *Col1a1*, which are markers of mesenchymal cells, were present in isolated hepatocytes. Subsequently, western blot analysis with anti-VNUT antibody recognized polypeptides with apparent molecular mass of 61 and 65 kDa (Fig. 1b). Immunohistochemical analysis indicated that VNUT immunoreactivity is localized with intracellular organelles, indicating presence of VNUT in hepatocytes (Fig. 1c). Double labeling immunofluorescence microscopy indicated that the VNUT immunoreactivity is partially co-localized with ApoB, a cargo of VLDL transport vesicles [24,25], with co-localization coefficients for VNUT: M1, 0.502; M2, 0.459, 6 determinations, but not with VAMP7, a marker for secretory vesicles, with co-localization coefficients for VNUT: M1, 0.115; M2, 0.306, 6 determinations; LAMP1, a marker for lysosome, with M1, 0.108; M2, 0.274, 5 determinations; EEA1, a marker for early endosome, with M1, 0.162; M2, 0.313, 5 determinations; and PDI, a marker for endoplasmic reticulum, with M1, 0.139; M2, 0.392, two determinations (Fig. 1d, insets). Histological analysis with HE staining showed no abnormality in the hepatic lobule structure in *Vnut*^{−/−} mice (Fig. 1e). Consistent with the localization of VNUT in hepatocytes, immunohistochemistry with anti-VNUT antibody revealed that a VNUT signal distributes throughout the hepatic lobule with relatively stronger in the hepatic perivenous region (Fig. 1e).

3.2. VNUT is involved in triglyceride secretion

Subsequently, we performed the direct measurement of ATP and triglyceride secretion from primary hepatocytes. In the presence of oleic acid, lipid droplets were made in the cytosol of primary hepatocytes (ESM Fig. 2). As shown in Fig. 2a, 25 mM glucose treatment stimulated the secretion of ATP from hepatocytes, which peaked at 10 min in WT mice, followed by the secretion of triglyceride in the medium (Fig. 2b). However, in *Vnut*^{−/−} mice, ATP release was blunted, and the triglyceride response was obviously suppressed.

We then hypothesized that extracellular nucleotides secreted by a VNUT-dependent mechanism stimulate triglyceride secretion via interaction with purinergic receptors on hepatocytes. To test our hypothesis, primary cultured hepatocytes were pretreated for 20 min with the following antagonists: 100 μ M of Suramin, a P2X receptor antagonist; 100 μ M of PPADS, a P2Y receptor antagonist; or 100 μ M of MRS2211, a P2Y13 receptor antagonist. Subsequently, the cells were stimulated by glucose for 60 min. Fig. 2c shows that none of the antagonists affected ATP secretion from hepatocytes. However, pretreatment with P2Y receptor antagonists, PPADS, and MRS2211 significantly suppressed triglyceride secretion, while pretreatment with the P2X antagonist did not change triglyceride secretion (Fig. 2d). Consistently 100 μ M of 2-methylthio-ADP, a selective agonist for P2Y1, P2Y12, and P2Y13, stimulated triglyceride secretion from WT as well as *Vnut*^{−/−} hepatocytes (Fig. 2e).

To obtain another line of evidence for participation of VNUT in triglyceride secretion from hepatocytes, the effect of clodronate, one of the 1st generation bisphosphonate known to be a specific inhibitor for VNUT, followed by inhibition of vesicular ATP release [21,22], was examined. As expected, 100 μ M of clodronate suppressed \sim 70% of glucose-dependent triglyceride secretion (Fig. 2e). The same

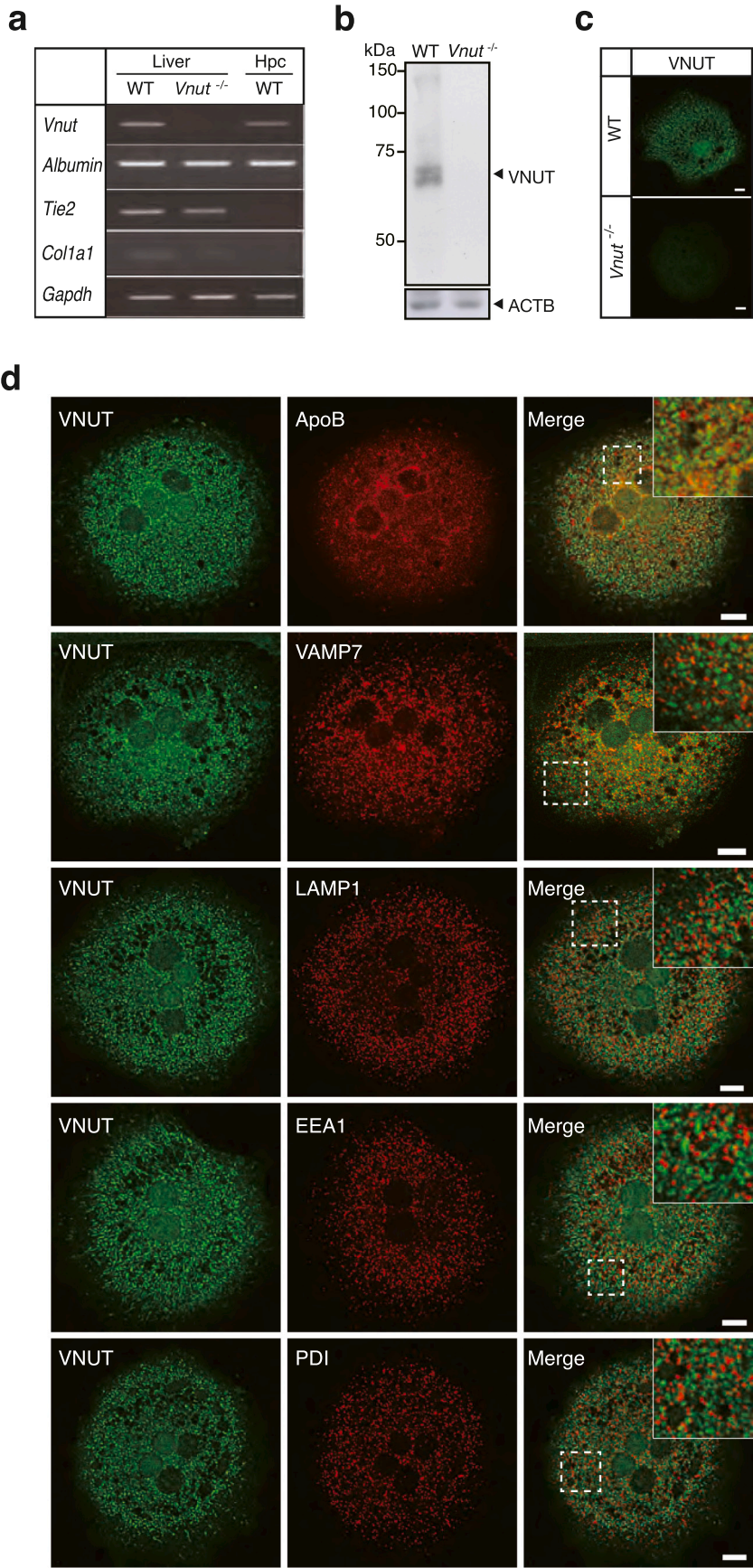


Fig. 1. Vesicular nucleotide transporter (VNUT) is expressed in hepatocytes. (a) Liver and isolated hepatocyte gene expression analyses from WT or *Vnut*^{-/-} mice fed a normal chow diet (NCD) for 12 weeks. Genes shown here include *Vnut*, a vesicular nucleotide transporter and hepatocyte marker; *Albumin*; mesenchymal cell markers including *Tie2*, a tyrosine kinase with Ig-like loops and epidermal growth factor homology domains-2 and *Col1a1*, a collagen type1 alpha1; and *Gapdh*, glyceraldehyde 3-phosphate dehydrogenase. Hpc, isolated hepatocytes. (b) Western blot analyses of microsomal fraction of hepatocytes (30 μg protein) from WT or *Vnut*^{-/-} mice using antibodies against VNUT. (c) Immunocytochemistry of isolated hepatocytes from WT or *Vnut*^{-/-} mice using VNUT antibody. Bars indicate 10 μm. (d) Isolated hepatocytes were double-immunostained with antibodies against VNUT (green, center panels) and organelle markers (ApoB for VLDL transport vesicles, VAMP7 for secretory vesicles, LAMP-1 for lysosomes, EEA1 for endosomes, PDI, for endoplasmic reticulum). Merged images (right panels) are shown. Bar = 10 μm. inset Higher magnification images of double-immunostained hepatocytes surrounded by a square in each picture of panel (c) were also shown as insets. (e) Hematoxylin and eosin (HE) staining and immunohistochemical analyses of the liver sections with VNUT antibody. DAB staining was used for visualization. Bars indicate 50 μm.

e

Fig. 1. (continued).

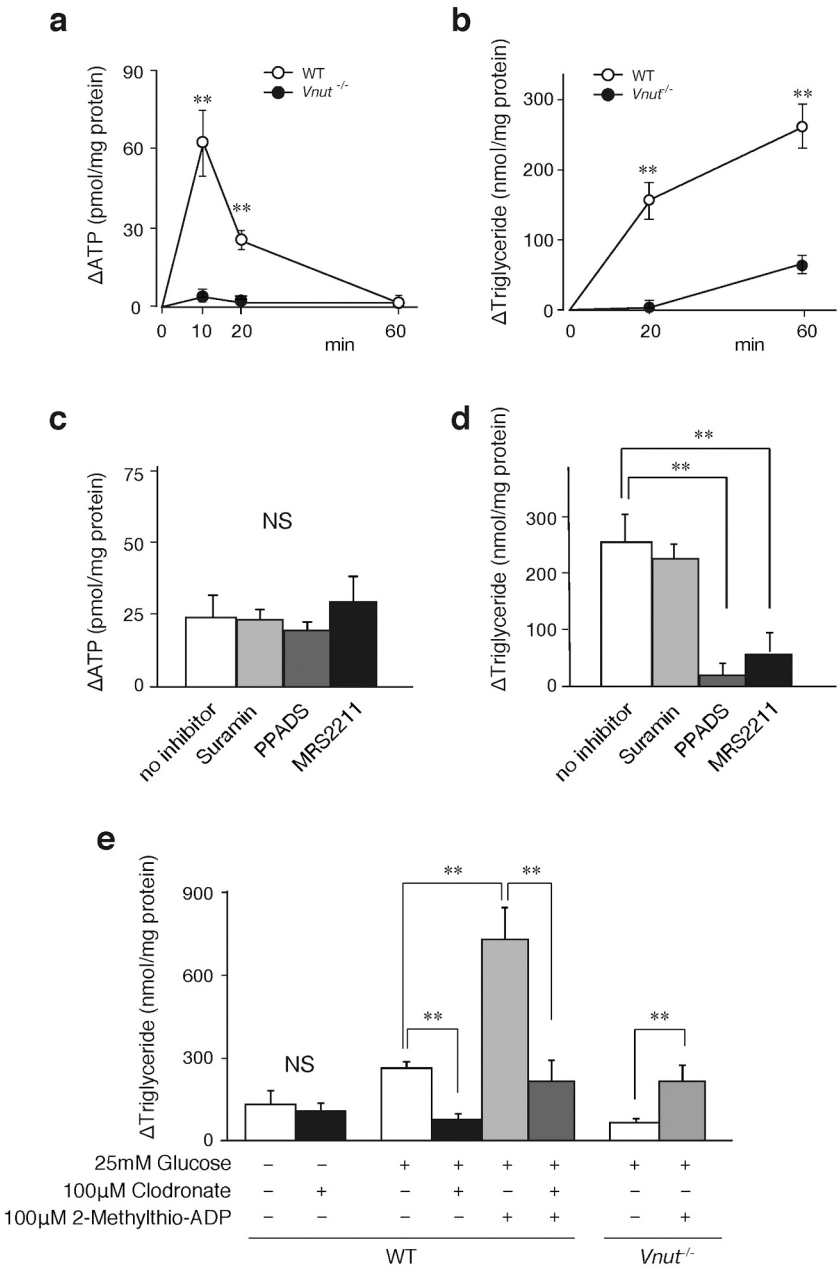
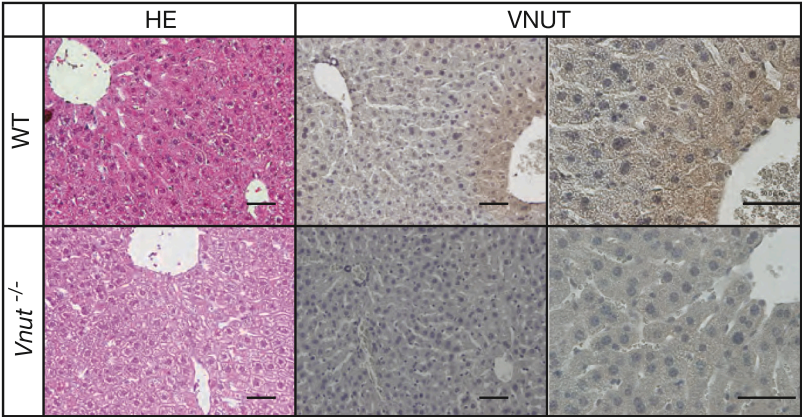


Fig. 2. VNUT helps hepatocytes to export triglycerides via P2Y receptors. (a, b) Primary cultured hepatocytes were stimulated with 25 mM glucose and incubated for 20 min, and the concentrations of ATP (a) and triglyceride (b) in the medium were then measured. Data are presented as the mean \pm standard error of mean (SEM); $n = 3$ mice; * $P < 0.05$, ** $P < 0.01$ (comparisons between genotype). (c, d) Primary cultured hepatocytes were pretreated with either 100 μ M of suramin (P2X receptor antagonist), 100 μ M of PPADS (pyridoxalphosphate-6-azophenyl-2',4'-disulfonic acid, a P2Y receptor antagonist), or 100 μ M of MRS2211 (2-[(2-chloro-5-nitrophenyl)azo]-5-hydroxy-6-methyl-3-[(phosphonoxy)methyl]-4-pyridinecarboxaldehyde disodium salt, a P2Y13 receptor antagonist) for 20 min. Subsequently, the cells were stimulated by glucose for 60 min, followed by the measurement of the ATP (c) and triglyceride (d) concentration in the medium. (e) Primary cultured hepatocytes prepared from WT or *Vnut*^{-/-} mice were stimulated by glucose for 60 min in the presence of 100 μ M clodronate and/or 100 μ M 2-methylthio-ADP. Then, triglyceride in the medium was quantified. In some experiments, hepatocytes were incubated in glucose free control medium (see ESM method) in the absence or presence of 100 μ M clodronate. Each value represents the mean \pm SEM. $n = 3$ mice; ** $P < 0.01$ vs. no inhibitor. NS, not significant.

concentration of clodronate also suppressed ~70% of glucose- and 2-methylthio-ADP-evoked triglyceride secretion (Fig. 2e). In the absence of glucose, about 30% level of triglyceride secretion was observed, which was less affected by the presence of clodronate at 100 μ M, indicating that the effect of clodronate on the basal triglyceride secretion was negligible (Fig. 2e). Taken together, these results suggest that VNUT-dependent vesicular ATP release and consequent activation of purinergic signaling through P2Y receptors promote glucose-induced triglyceride secretion from hepatocytes.

3.3. Role of VNUT in the hepatic lipid metabolism

Purinergic signaling is known to involve in lipid metabolism [26,27]. Therefore, we investigated the role of VNUT on the hepatic lipid profile. As shown in Fig. 3a and b, oil red O staining in WT hepatocytes decreased ~90% after re-feeding for 4 h. In *Vnut*^{-/-} hepatocytes, however, ~50% oil red O staining remained after re-feeding for 4 h. Consistent with the observation with oil red O staining, the hepatic triglyceride content was significantly reduced to less than 50% in the WT liver, but not in the *Vnut*^{-/-} liver after re-feeding for 4 h (Fig. 3c).

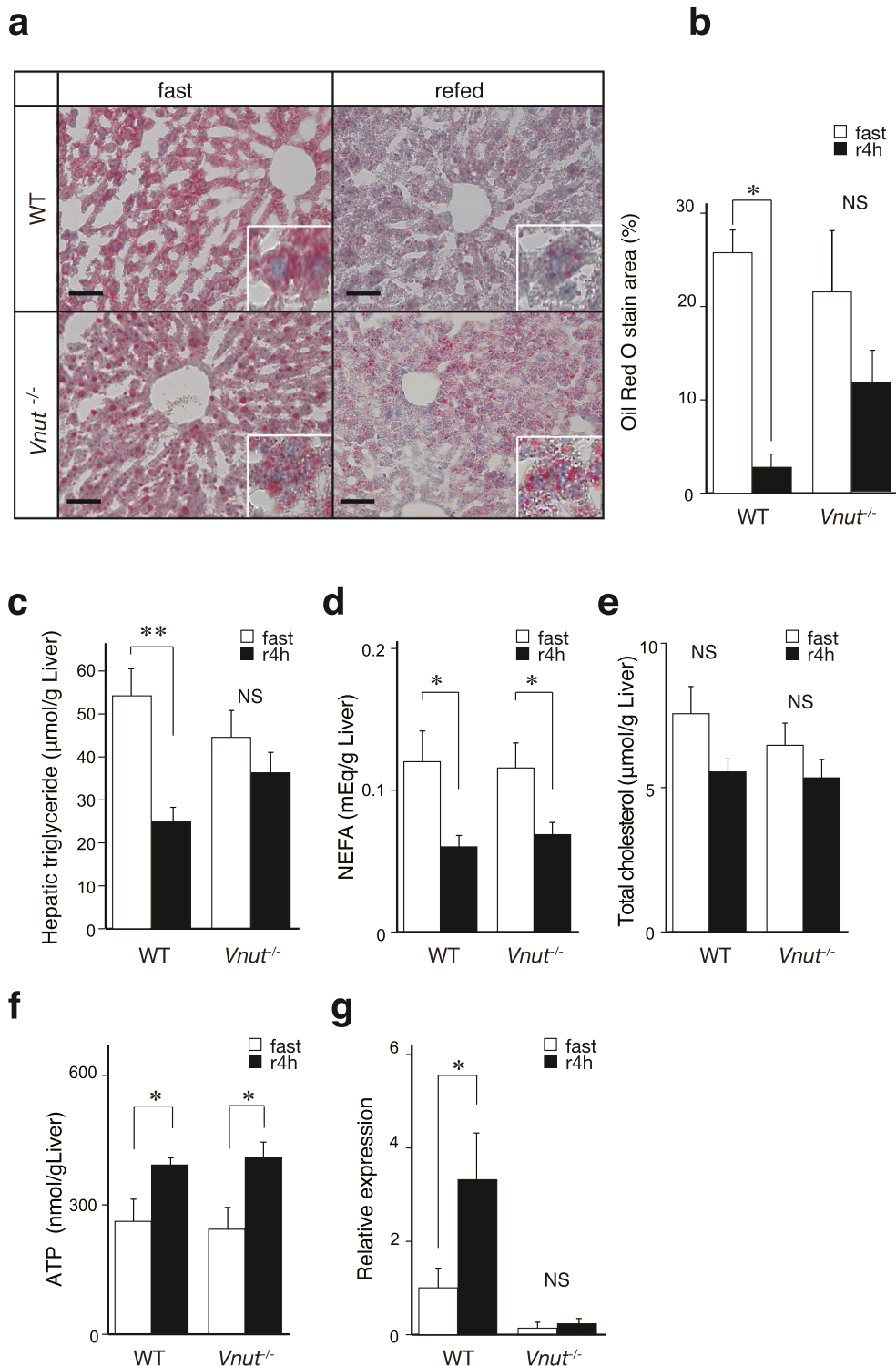


Fig. 3. Hepatic lipid, ATP content, and *Vnut* expression changed by the meal state. (a) Representative oil red O staining of the liver sections in 10-week-old mice. Bars indicate 50 μ m. (b) Semiquantitative presentation of oil red O staining. Area of oil red O staining of three independent sections was measured by image j. (c–e) Hepatic triglycerides (c), NEFAs (d), and total cholesterol (e) content after an 18-h fast (fast) and followed by refeeding for 4 h (r4h). Data are presented as the mean \pm standard error of the mean (SEM); $n = 8$ per group; 9–10-week-old mice. * $P < 0.05$; NS, not significant (comparisons between fasting and refed). (f) ATP content extracted from the liver. Data are presented as the mean \pm SEM; $n = 3$ –4 mice per group. (g) Liver gene expression analysis of *Vnut*. Data are presented as the mean \pm SEM. $n = 5$; * $P < 0.05$ (comparisons between fasting and refed).

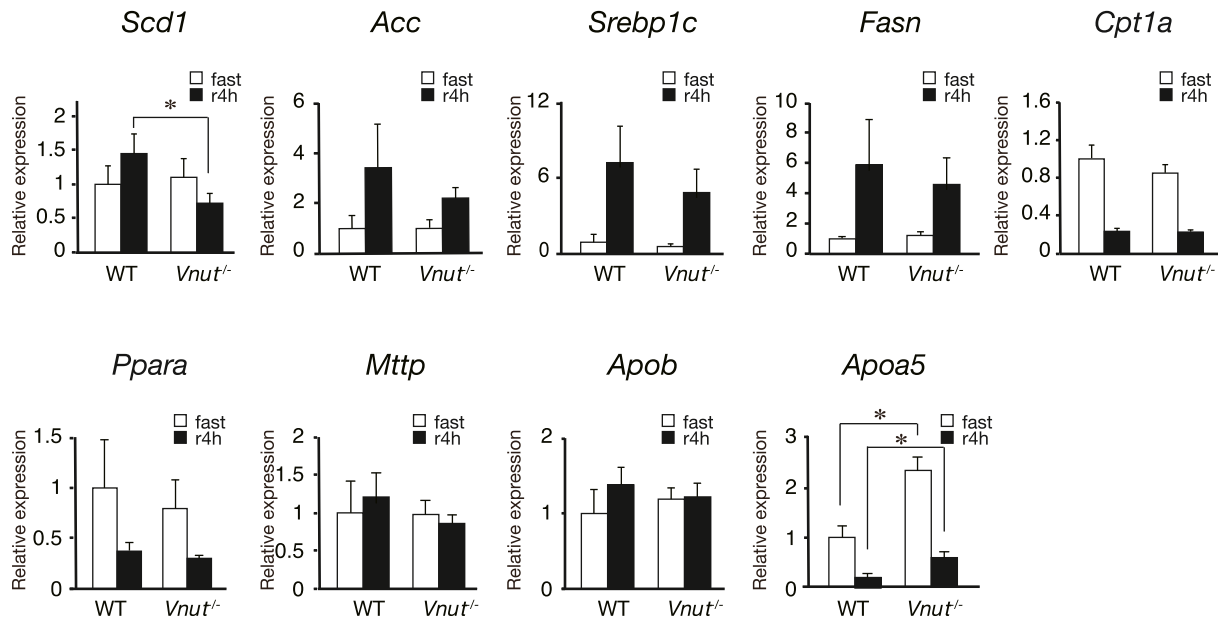


Fig. 4. VNUT is involved in lipid metabolism. Liver gene expression analyses from WT or *Vnut*^{-/-} mice. Samples were collected after an 18-h fast (fast) or after refeeding for 4 h (r4h). mRNA levels of the genes (*Scd1*, stearoyl-CoA desaturase-1; *Acc*, acetyl-CoA carboxylase; *Srebp1c*, sterol regulatory element-binding protein; *Fasn*, fatty acid synthase; *Cpt1a*, carnitine palmitoyltransferase 1a; *Ppara*, peroxisome proliferator-activated receptor alpha; *Mttp*, microsomal triglyceride transfer protein; *Apob*, Apolipoprotein b; *Apoa5*, ApolipoproteinA-V) are shown. mRNA expression was normalized to *Gapdh*, and hepatic gene expression in WT mice was set as equal to one. Data are presented as the mean \pm SEM. $n = 5$ mice per group. * $P < 0.05$ (comparisons between genotypes).

Hepatic NEFA content decreased after re-feeding in both genotypes (Fig. 3d). No change was observed in total cholesterol storage between genotypes (Fig. 3e). Re-feeding for 4 h increased hepatic ATP levels in both genotypes, indicating that VNUT is dispensable for ATP synthesis (Fig. 3f). Re-feeding also increased *Vnut* expression 3.3-fold in quantitative RT-PCR analysis (Fig. 3g). Taken together, these results suggest that VNUT plays an important role in postprandial release of triglyceride from hepatocytes.

To better understand the impact of *Vnut* gene expression, a microarray experiment was performed using mRNA prepared from WT and *Vnut*^{-/-} mouse livers. Gene ontology analysis revealed that the genes on antigen processing via major histocompatibility complex II, lipid metabolism, and inflammatory response were down-regulated in the liver of *Vnut*^{-/-} mice (ESM Fig. a). There were several changes in the gene cluster for the lipid metabolic process. Expression of genes involved in lipogenesis such as *Scd1*, *Fasn*, *Elovl3*, *Srebf1*, and *Insig1* in *Vnut*^{-/-} mice was lower compared with WT mice. *Scd1* and *Elovl3* participate in desaturation and extension of fatty acids, playing roles in the synthesis of long chain polyunsaturated fatty acids. *Srebf1* and *Insig1* are required for cholesterol and fatty acid biosynthesis. In contrast, genes involved in lipolysis such as *Apoa5* and *Fgf21* in *Vnut*^{-/-} were higher compared with WT in the refed state (ESM Fig. 3b). APOA5 activates lipoprotein lipase (LPL) to facilitate the hydrolyzation of fatty acids and promotes lipid droplet accumulation in hepatocytes [28]. FGF21 is induced by fasting and lowers triglyceride level [29]. These results suggest that VNUT affects lipid metabolism through dynamic change of gene expression profiles involved mainly in lipogenesis in the liver.

Next, we performed quantitative RT-PCR analyses using mRNA prepared from livers from fasting or re-fed WT or *Vnut*^{-/-} mice as shown in Fig. 4. Regarding to the fatty acid synthesis, *Scd1* expression was significantly suppressed after re-feeding for 4 h in *Vnut*^{-/-} mice. *Acc*, *Srebp1c*, and *Fasn* mRNA levels showed a trend to be lower in *Vnut*^{-/-} mice after re-feeding. The expression of the genes for fatty acid oxidation, *Cpt1a* and *Ppara*, were not different between the genotypes. The expression of the genes involved in VLDL formation, *Mttp* and *Apob*, were not different as well. On the other hand, *Apoa5* expression was found to be significantly higher in *Vnut*^{-/-} compared with WT

regardless of the feeding state.

We then examined blood samples to explore the role of VNUT in lipid profile *in vivo*. Serum triglyceride levels after an 18-h fast showed no significant difference between the genotypes (Fig. 5a). After re-feeding for 4 h, serum triglyceride levels showed a rapid and dramatic increase in WT mice but not in *Vnut*^{-/-} mice. Glucose (Fig. 5a), total cholesterol, and NEFA profiles (ESM Fig. 4a) showed no significant difference between the genotypes. Serum triglyceride levels reflect the balance between lipoprotein clearance by LPL and lipoprotein secretion. To evaluate hepatic triglyceride secretion, 18-h fasted mice were injected with tyloxapol, an LPL inhibitor. As shown in Fig. 5b, the serum triglyceride level 4 h after injection was significantly inhibited in *Vnut*^{-/-} mice. The triglyceride secretion rate in *Vnut*^{-/-} mice was suppressed to less than half of that in WT mice. In tyloxapol injection experiments, cholesterol, and NEFA levels did not differ between the genotypes (ESM Fig. 4b). Taken together, these results suggest that a defect in postprandial triglyceride increase can be attributed to impaired triglyceride secretion in *Vnut*^{-/-} mice, which are in good agreement with the *in vitro* phenotype as described in Fig. 2.

3.4. VNUT exacerbates steatohepatitis in mice fed a HFD

Finally, we investigated the role of VNUT in the progression of steatohepatitis, because purinergic signaling initiated by extracellular nucleotide induces inflammation [13], and vesicular ATP release actually affects lipid metabolism as describe above. As shown in Fig. 6a, it was found a lower serum triglyceride level and higher hepatic triglyceride content in *Vnut*^{-/-} mice as compared with those in WT mice (Fig. 6a, b). HFD increased *Vnut* mRNA level by 3.4-fold in WT liver (Fig. 6c). Increased VNUT immunoreactivity in liver sections of refeeding of NCD was also observed (Fig. 6d), consistent with expression of *Vnut* (Fig. 3g). More pronounced expression of VNUT immunoreactivity was observed in liver sections of HFD-fed mice (Fig. 6d). Under the HFD conditions, HE staining demonstrated that the WT liver contained macrovesicular lipid droplets in the perivenous zone (Fig. 6e, left panels). In contrast, the *Vnut*^{-/-} liver had many macrovesicular lipid droplets in both the perivenous and periportal zones, which is consistent

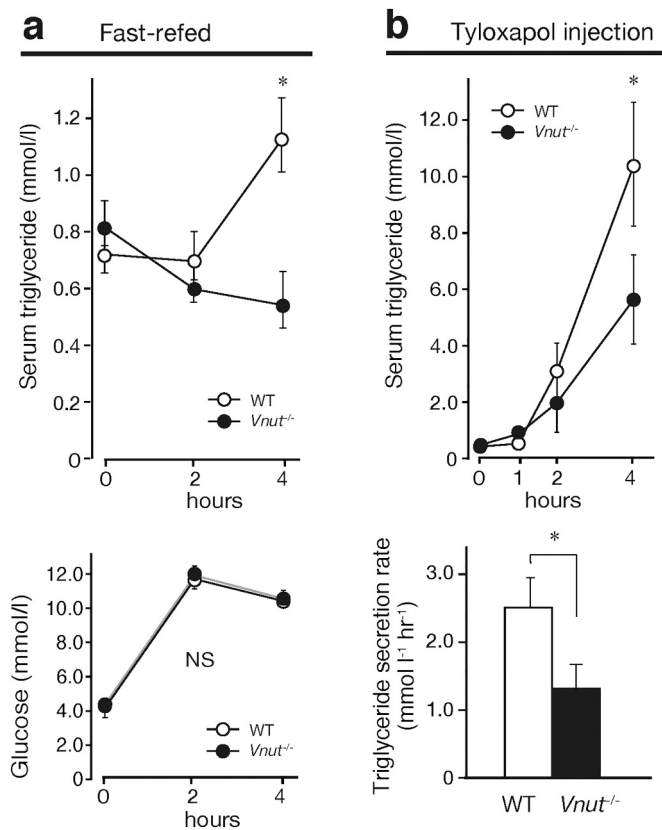


Fig. 5. Postprandial triglyceride level did not increase in *Vnut*^{-/-} mice because of impaired triglyceride secretion. (a) Serum triglyceride and glucose profiles of 8-week-old mice during a 4-h refeed after an 18-h fast. Data are presented as the mean \pm SEM; $n = 17$ –20; * $P < 0.05$; NS, not significant (comparisons between genotypes). (b) Hepatic triglyceride secretion was assessed by the measuring serum triglyceride levels after administration of tyloxapol. Data are presented as the mean \pm SEM. $n = 8$; * $P < 0.05$.

with the increased triglyceride content in the liver of *Vnut*^{-/-} mice (Fig. 6e, right panels). Microvesicular steatosis and ballooned hepatocytes were observed in the perivenous zone in livers of both genotypes. However, intralobular inflammatory foci, which are characteristic of NASH, were frequently observed in the WT liver (Fig. 6e, left lower panel, arrows), but not in the *Vnut*^{-/-} liver. We performed pathological grading of the liver using the NAFLD activity score [23]. The steatosis score was higher in *Vnut*^{-/-} mice compared with WT mice, in agreement with the increased hepatic triglyceride content (Fig. 6b, f). On the other hand, the lobular inflammation score was significantly lower in *Vnut*^{-/-} mice, although the ballooning scores were comparable with WT mice (Fig. 6f).

Serum AST and ALT levels, reflecting liver cell damage, were significantly lower in *Vnut*^{-/-} mice (Fig. 7a). Therefore, we analyzed the expression of genes involved in inflammation and fibrosis. As shown in Fig. 7b, qRT-PCR analyses showed that expression of *Emr1*, also known as F4/80, which is an activated macrophage marker, was significantly reduced in *Vnut*^{-/-} mice. There was no statistical change in the *Mcp-1* level (Fig. 7b). F4/80 immunostaining revealed that there were significantly fewer activated macrophages in the *Vnut*^{-/-} liver compared with the WT liver (Fig. 7c). *Timp1* and *Col1a1* levels in *Vnut*^{-/-} mice were lower (Fig. 7d), and the *Tgfb* level showed a lower trend in *Vnut*^{-/-} compared with WT ($P = 0.06$). We performed Picrosirius Red staining to investigate fibrosis in the liver sections. As shown in Fig. 7e, *Vnut*^{-/-} livers showed much weaker staining than WT livers. Thus, *Vnut*^{-/-} mice on a HFD showed a fatty liver with less inflammation and fibrosis, suggesting that VNUT has an important role in the progression of diet-induced steatohepatitis through activating the purinergic signaling.

4. Discussion

In the present study, we reported for the first time that VNUT is expressed in hepatocytes and plays an important role in postprandial triglyceride secretion. Presence of VNUT in hepatocytes were verified by real-time PCR, Western blot and indirect immunofluorescence microscopy with isolated hepatocytes and VNUT-specific probes. Presence of VNUTs with different molecular mass in SDS gel electrophoresis may be due to existence of two different isoforms [30]. Double labeling immunohistochemistry indicated that VNUT immunoreactivity is partially colocalized with apoB, but not with VAMP7, LAMP1, EEA1, and PDI, suggesting that VNUT is associated with VLDL-containing secretory vesicles. As shown in Fig. 8, these results assume that hepatocytes have accumulated ATP in VLDL-containing secretory vesicles, an organelle involving in secretion of VLDL from hepatocytes [24,25], and that ATP and VLDL are co-stored and co-released. Although further studies will be necessary to identify and characterize the VNUT-containing organelles in hepatocytes, this assumption explains well the mode of action of ATP as an autocrine or paracrine signal transmitter in the regulation of VLDL secretion as described below.

Our *in vitro* study demonstrated that ATP is released via VNUT-mediated vesicular release from hepatocytes upon glucose stimulation, followed by the secretion of triglyceride. This triglyceride secretion was suppressed by pharmacological inhibition of VNUT as well as P2Y13 receptor, suggesting that vesicular ATP release mediated by VNUT promotes triglyceride-rich lipoprotein secretion via P2Y13 receptor in an autocrine and/or paracrine manner. *In vivo* long-term HFD feeding experiment revealed that *Vnut*^{-/-} mice were protected from diet-induced hepatic inflammation as well as fibrosis, despite the increased triglyceride accumulation in the liver.

Chatterjee et al., reported that ADP stimulate P2Y13 receptor on hepatocytes to promote the secretion of APOB100, a major component of VLDL, and to inhibit insulin signaling and the secretion of APOA-I, an HDL apolipoprotein [27]. They suggested that high circulatory nucleotide, induced by elevated blood glucose, might block hepatic APOA-I secretion while stimulate APOB100 output in insulin resistant patients. In good agreement with this, our results suggested that upon glucose stimulation, hepatocytes themselves drive vesicular ATP release via VNUT to stimulate the secretion of VLDL, the principal vehicle for the transport of endogenous triglyceride (Fig. 8). Given that hepatocytes secrete triglycerides in the fed state to stock lipids in peripheral adipose tissue, it may be reasonable that VLDL is synthesized and secreted at a higher rate in perivenous compared with periportal hepatocytes [31]. Because of metabolic zonation in the liver, strong expression of VNUT in the perivenous region may have an advantage for secreting VLDL after meals (Fig. 1e). In line with this, it is reasonable that more than three-fold increase of *Vnut* expression (Fig. 3g, Fig. 6c) as well as increase of VNUT immunoreactivities (Fig. 6d) were observed after refeeding or HFD feeding. An excess amount of VLDL secretion leads to postprandial hypertriglyceridemia and increases the risk of the cardiovascular disease. Therefore, it is important to establish a strategy for normalization of postprandial hypertriglyceridemia that prevents arteriosclerotic disease, and VNUT may be involved in this process.

In our study, *Apoa5* expression remained at a high level even after refeeding in *Vnut*^{-/-} mice. APOA5 is known to enhance the catabolism of triglyceride-rich lipoproteins by LPL in plasma and to inhibit the rate of production of VLDL in hepatocytes [32,33]. Overexpression of *ApoA5* is reported to markedly reduce the level of plasma triglyceride and to facilitate hepatic triglyceride accumulation in mice [34]. In addition to direct inhibition of triglyceride secretion from hepatocytes through the blockade of P2Y13 receptor signaling, increased fat accumulation and reduced postprandial serum triglyceride levels in *Vnut*^{-/-} mice might be in part explained by increased *Apoa5* expression. A further examination is required to reveal the role of VNUT in hepatic triglyceride metabolism.

While simple steatosis remains free of inflammation in most cases, a

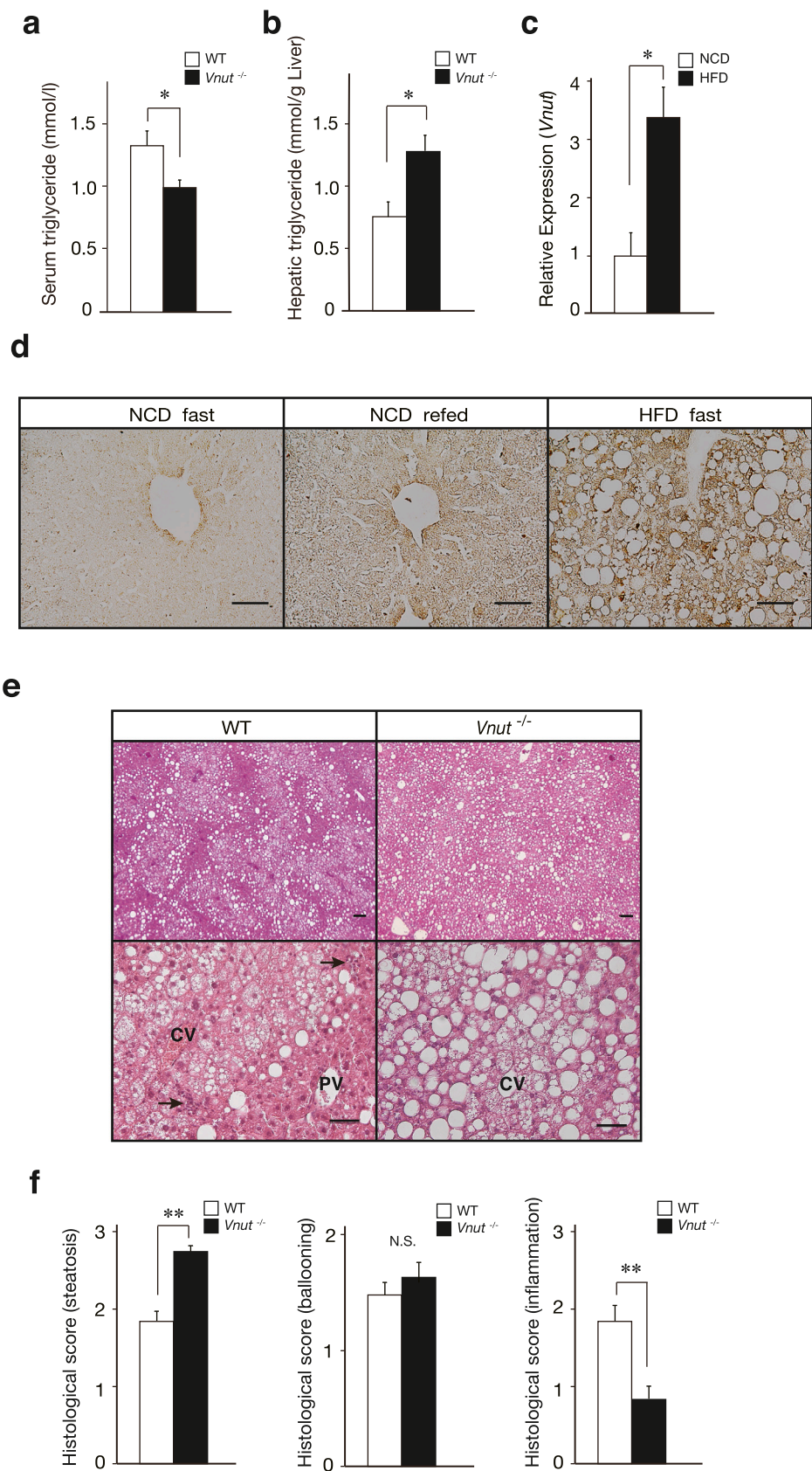


Fig. 6. VNUT regulates the lipid profile in mice fed a high-fat diet. (a) Serum triglyceride level and (b) hepatic triglyceride content after an 18 h of fasting. Mice were fed an HFD for 48 weeks. Values are presented as the mean \pm standard error of the mean (SEM); $n = 5$; * $P < 0.05$. (c) Liver gene expression analyses of *Vnut* from livers of either NCD-fed (NCD) or HFD-fed (HFD) WT mice. Data are presented as the mean \pm SEM. $n = 5$; * $P < 0.05$. (d) Immunohistochemical analyses of the liver sections with VNUT antibody (*left*) liver from fasted NCD-fed WT mouse; (*center*) liver from re-fed NCD-fed WT mice; (*right*) liver from fasted HFD-fed WT mice. Bar = 50 μ m. (e) Representative HE staining in the liver section in WT and *Vnut*^{-/-} mice fed a HFD for 48 weeks. Bars in upper and lower panels indicate 50 and 100 μ m, respectively. Arrows indicate inflammatory foci. CV, central vein; PV, portal vein. (f) Histological scoring of NASH in liver sections in (e). Steatosis and inflammation were scored using a 0–3 scale while ballooning was scored using a 0–2 scale in accordance with the NASH Clinical Research Network Committee scoring system ($n = 3$, at least 10 slides per each mouse). Data are expressed as the mean \pm SEM. ** $P < 0.01$.

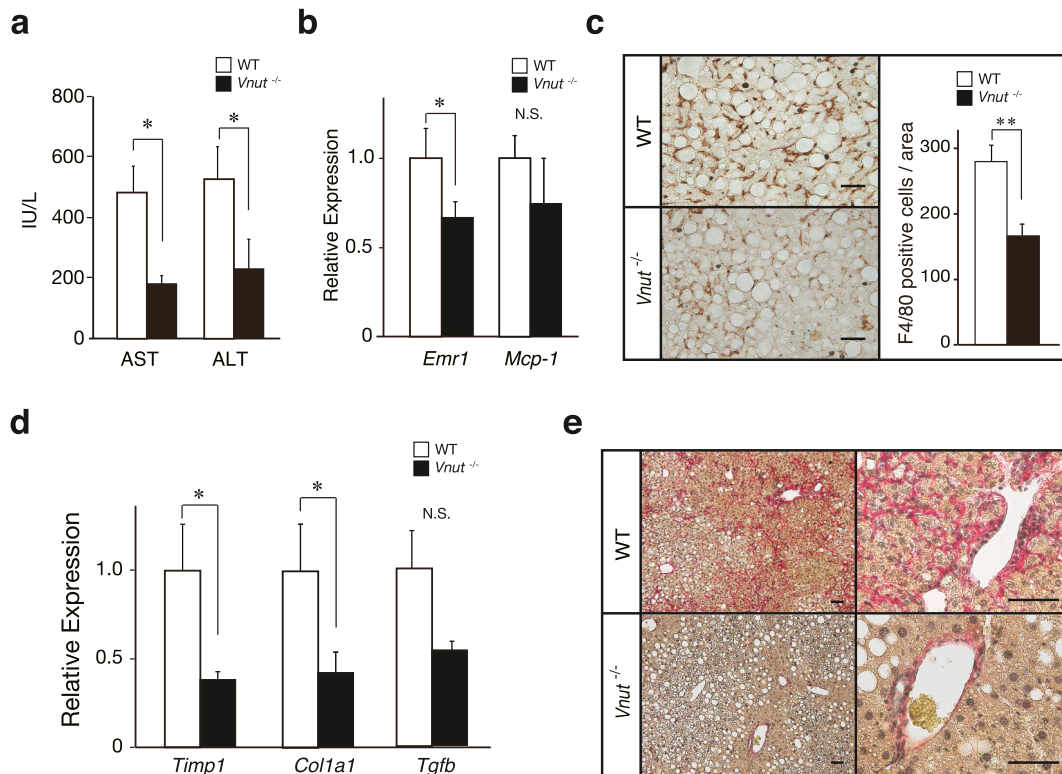


Fig. 7. Decreased liver damage and steatohepatitis in *Vnut*^{-/-} mice fed a HFD. (a) Serum alanine aminotransferase (ALT) and aspartate aminotransferase (AST) levels in mice fed a HFD for 48 weeks. Data are presented as the mean \pm SEM; $n = 4$; * $P < 0.05$ (comparison between genotypes). (b) Liver gene expression analyses from WT or *Vnut*^{-/-} mice fed a HFD for 48 weeks. Shown are mRNA levels of genes related to macrophage activity (*Emr1*, epidermal growth factor-like module-containing mucin-like hormone receptor-like 1; *Mcp-1*, monocyte chemoattractant protein-1). mRNA expression was normalized against *Gapdh*, and the gene expression in livers from WT mice was set as equal to one. Data are presented as the mean \pm SEM; $n = 5$; * $P < 0.05$; N.S.; not significant. (c) Representative immunohistochemistry using F4/80 antibody in the liver sections. Bars indicate 50 μ m. Quantitative analysis of F4/80-positive cells is shown in the right panel. Data are presented as the mean \pm SEM; $n = 5$; ** $P < 0.01$. (d) Liver gene expression analyses. mRNA levels of genes related to fibrosis are shown (*Timp1*, tissue inhibitor of metalloproteinase; *Tgfb*, transforming growth factor beta; *Col1a1*, collagen type1 alpha1). mRNA expression was normalized against *Gapdh*, and the gene expression of livers from WT mice was set as 1. Data are presented as the mean \pm SEM; $n = 5$; * $P < 0.05$. (e) Representative Picrosirius Red staining in the liver sections. Bars indicate 50 μ m.

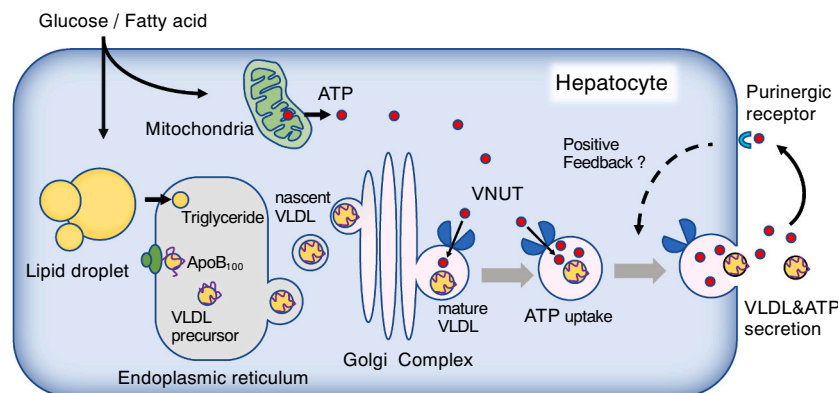


Fig. 8. Schematic presentation on the mechanism of VNUT-mediated secretion of ATP from hepatocytes. Hepatocytes may store ATP in VLDL-containing secretory vesicles and co-secrete ATP and VLDL upon glucose stimulations. Released ATP may act an intercellular signaling molecule as an autocrine- or paracrine fashion, and regulate secretion of VLDL.

small group of patients develops inflammation and fibrosis, which may be promoted by many parallel hits including inflammatory mediators derived from various tissues [35]. Many potential hits (e.g. oxidative stress, lipotoxicity, endotoxin, endoplasmic reticulum stress, and insulin resistance) have been derived from the gut and the adipose tissue. ATP and certain nucleotides also serve as host-derived danger signals and modulate the immune and inflammatory response [4,36]. In the liver,

macrophages, especially Kupffer cells, are known to play a role in enhancing inflammation and promoting fibrosis through comprehensive interactions with not only hepatocytes but also mesenchymal cells such as hepatic stellate cells [37]. It is thus possible that ATP secreted by hepatocytes activates both macrophages and hepatic stellate cells to enhance inflammation and fibrosis. Consistent with the idea, Kupffer cells and hepatic stellate cells also release ATP, although the releasing

mechanisms remain unknown [38,39]. Biliary epithelial cells in the liver are also known to secrete ATP through exocytosis of VNUT-containing vesicles [40]. Moreover, we reported that macrophages and neutrophils secrete ATP in a VNUT dependent fashion [16,21,41–43]. In any events, VNUT may mediate the ATP-dependent intercellular communication between hepatocytes and non-hepatocytes in the liver to promote the progression of hepatic inflammation and fibrosis. To clarify the intercellular communication that takes place during NASH progression between hepatocytes and non-hepatocytes in the liver, tissue and/or hepatocyte-specific deletion of VNUT might be required. Such study is currently in progress in our laboratory. Nonetheless, in our study, histological evaluation revealed significantly lower activated macrophage levels and lower collagen deposition in the liver of *Vnut*^{-/-} mice under HFD conditions (Fig. 7).

It is noteworthy that high glucose-stimulated triglyceride release from hepatocytes was inhibited by a VNUT inhibitor, clodronate (Fig. 2e) [22]. Because clodronate blocks ATP-dependent secretion of inflammatory cytokines such as interleukin-6 and tumor necrosis factor- α at very low concentration *in vivo*, followed by suppression of inflammation [22], it is reasonable to speculate that clodronate has pharmacological effects on NASH that have similar pathology to VNUT gene knockout mice. Indeed, we found that low concentration of clodronate is effective to block progression of steatohepatitis (Hasuzawa et al., submitted elsewhere).

In conclusion, the present study provided the evidence that VNUT is a key player in postprandial triglyceride release and in progression of steatohepatitis. Under conditions of energy excess, purinergic signaling induced by VNUT in the liver may exacerbate metabolic diseases such as NASH. VNUT is a molecule that links a metabolic disorder with inflammation. Therefore, VNUT could be a novel target for intervention in metabolic diseases such as NASH.

Funding sources

This work was supported in part by the Japan Society for the Promotion of Science (JSPS) KAKENHI (M. Nomura, Grant Number 17K09885; Y. Moriyama, Grant Number 18H02407) and Grants-in-Aid for Research.

CRediT authorship contribution statement

Keita Tatsushima: Methodology, Investigation, Formal analysis, Writing - original draft. **Nao Hasuzawa:** Methodology, Investigation, Formal analysis, Writing - original draft. **Lixiang Wang:** Investigation. **Miki Hiasa:** Methodology, Investigation, Writing - original draft. **Shohei Sakamoto:** Investigation. **Kenji Ashida:** Formal analysis. **Nobuyuki Sudo:** Formal analysis. **Yoshinori Moriyama:** Methodology, Formal analysis, Writing - original draft, Supervision, Funding acquisition. **Masatoshi Nomura:** Methodology, Investigation, Formal analysis, Writing - original draft, Supervision, Funding acquisition.

Declaration of competing interest

The authors declare that they have no known competing financial interests or personal relationships that could have appeared to influence the work reported in this paper.

Acknowledgments

The authors thank Drs. H Omote and T Miyaji (Okayama University) for helpful discussions at early stage of the study. The authors also thank the Research Support Center, Graduate School of Medical Science, Kyushu University, for technical support. Additionally, we thank Jodi Smith, PhD, from Edanz Group (<https://en-author-services.edanzgroup.com/>) for editing a draft of this manuscript.

Appendix A. Supplementary data

Supplementary data to this article can be found online at <https://doi.org/10.1016/j.bbadis.2020.166013>.

References

- [1] V.W. Wong, S. Chitturi, G.L. Wong, J. Yu, H.L. Chan, G.C. Farrell, Pathogenesis and novel treatment options for non-alcoholic steatohepatitis, *Lancet Gastroenterol Hepatol* 1 (2016) 56–67.
- [2] G.S. Hotamisligil, Inflammation and metabolic disorders, *Nature* 444 (2006) 860–867.
- [3] G. Burnstock, Physiology and pathophysiology of purinergic neurotransmission, *Physiol. Rev.* 287 (2009) 659–797.
- [4] G. Burnstock, B. Vaughn, S.C. Robson, Purinergic signalling in the liver in health and disease, *Purinergic Signal* 10 (2014) 51–70.
- [5] H. Zimmermann, M. Zebisch, N. Strater, Cellular function and molecular structure of ecto-nucleotidases, *Purinergic Signal* 8 (2012) 437–502.
- [6] S. Dolovcak, S.L. Waldrop, F. Xiao, G. Kilic, Evidence for sustained ATP release from liver cells that is not mediated by vesicular exocytosis, *Purinergic Signal* 7 (2011) 435–446.
- [7] A.P. Feranchak, M.A. Lewis, C. Kresge, et al., Initiation of purinergic signaling by exocytosis of ATP-containing vesicles in liver epithelium, *J. Biol. Chem.* 285 (2010) 8138–8147.
- [8] Fitz J. Gregory, Regulation of cellular ATP release *Trans Am Clin Association* 118 (2007) 199–208.
- [9] A.P. Feranchak, G. Fitz, R.M. Roman, Volume-sensitive purinergic signaling in human hepatocytes, *J. Hepatol.* 33 (2000) 174–182.
- [10] K. Enjoji, K. Kotani, C. Thukral, et al., Deletion of *cd39/entpd1* results in hepatic insulin resistance, *Diabetes* 57 (2008) 2311–2320.
- [11] D.J. Friedman, M.E. Talbert, D.W. Bowden, et al., Functional ENTPD1 polymorphisms in African Americans with diabetes and end-stage renal disease, *Diabetes* 58 (2009) 999–1006.
- [12] M.H. Garcia-Hernandez, L. Portales-Cervantes, N. Cortez-Espinosa, et al., Expression and function of P2X2 receptor and CD39/Entpd1 in patients with type 2 diabetes and their association with biochemical parameters, *Cell. Immunol.* 269 (2011) 135–143.
- [13] D.L. Sparks, C. Chatterjee, Purinergic signaling, dyslipidemia and inflammatory disease, *Cell. Physiol. Biochem.* 30 (2012) 1333–1339.
- [14] K. Sawada, N. Echigo, N. Juge, et al., Identification of a vesicular nucleotide transporter, *Proc. Natl. Acad. Sci. U. S. A.* 105 (2008) 5683–5686.
- [15] S. Sakamoto, T. Miyaji, M. Hiasa, et al., Impairment of vesicular ATP release affects glucose metabolism and increases insulin sensitivity, *Sci. Rep.* 4 (2014) 6689.
- [16] Y. Moriyama, M. Hiasa, S. Sakamoto, H. Omote, M. Nomura, Vesicular nucleotide transporter (VNUT): appearance of an actress on the stage of purinergic signaling, *Purinergic Signal* 13 (2017) 387–404.
- [17] J. Folch, M. Lees, G.H.S. Stanley, A simple method for the isolation and purification of total lipides from animal tissues, *J. Biol. Chem.* 226 (1957) 497–509.
- [18] J. Chida, K. Yamane, T. Takei, H. Kido, An efficient extraction method for quantitation of adenosine triphosphate in mammalian tissues and cells, *Anal. Chim. Acta* 727 (2012) 8–12.
- [19] Q. Wang, S. Li, L. Jiang, et al., Deficiency in hepatic ATP-citrate lyase affects VLDL-triglyceride mobilization and liver fatty acid composition in mice, *J. Lipid Res.* 51 (2010) 2516–2526.
- [20] R.A. Felix, S. Martin, S. Pinion, D.J. Crawford, Development of a comprehensive set of P2 receptor pharmacological research compounds, *Purinergic Signaling* 8 (2012) S101–S112.
- [21] Y. Kato, M. Hiasa, R. Ichikawa, et al., Identification of a vesicular ATP release inhibitor for the treatment of neuropathic and inflammatory pain, *Proc. Natl. Acad. Sci. U. S. A.* 114 (2017) E6297–E6305.
- [22] Y. Moriyama, M. Nomura, Clodronate: a vesicular ATP release blocker, *Trends Pharmacol. Sci.* 39 (2018) 13–23.
- [23] D.E. Kleiner, E.M. Brunt, M. Van Natta, et al., Nonalcoholic Steatohepatitis clinical research network, Design and validation of a histological scoring system for nonalcoholic fatty liver disease. *Hepatology* 41 (2005) 1313–1321.
- [24] S.A. Siddiqi, VLDL exits from the endoplasmic reticulum in a specialized vesicle, the VLDL transport vesicle, in rat primary hepatocytes, *Biochem. J.* 413 (2008) 333–342.
- [25] T. Hossain, A. Riad, S. Siddiqi, S. Parthasarathy, S.A. Siddiqi, Mature VLDL triggers the biogenesis of a distinct vesicle from the *trans*-Golgi network for its export to the plasma membrane, *Biochem. J.* 459 (2014) 47–58.
- [26] L.O. Martinez, S. Jacquet, J.-P. Esteve, et al., Ectopic beta-chain of ATP synthase is an apolipoprotein A-I receptor in hepatic HDL endocytosis, *Nature* 421 (2003) 75–79.
- [27] C. Chatterjee, D.L. Sparks, Extracellular nucleotides inhibit insulin receptor signaling, stimulate autophagy and control lipoprotein secretion, *PLoS One* 7 (2012), e36916.
- [28] S.K. Nilsson, J. Heeren, G. Olivecrona, M. Merkel, Apolipoprotein A-V; a potent triglyceride reducer, *Atherosclerosis* 219 (2011) 15–21.
- [29] S.A. Kliewer, D.J. Mangelsdorf, A dozen years of discovery: insights into the physiology and pharmacology of FGF21, *Cell Metab.* 29 (2019) 246–253.
- [30] J.I. Sesma, S.M. Kreda, S.F. Okada, C. van Heusden, L. Moussa, L.C. Jones, W. K. O'Neal, N. Togawa, M. Hiasa, Y. Moriyama, E.R. Lazarowski, Vesicular

- nucleotide transporter regulates the nucleotide content in airway epithelium mucin granules, *Am. J. Phys.* 304 (2013) C976–C984.
- [31] M. Guzmán, J. CASTRO, Zonation of fatty acid metabolism in rat liver, *Biochem. J.* 264 (1989) 107–113.
- [32] M. Garelnabi, K. Lor, J. Jin, F. Chai, N. Santanam, The paradox of ApoA5 modulation of triglycerides: evidences from clinical and basic research, *Clin. Biochem.* 46 (2013) 12–19.
- [33] L.A. Pennacchio, M. Olivier, J.A. Hubacek, et al., An apolipoprotein influencing triglycerides in humans and mice revealed by comparative sequencing, *Science* 294 (2001) 169–173.
- [34] X. Shu, L. Nelbach, R.O. Ryan, T.M. Forte, Apolipoprotein A-V associates with intrahepatic lipid droplets and influences triglyceride accumulation, *Biochim. Biophys. Acta* 1801 (2010) 605–608.
- [35] H. Tilg, A.R. Moschen, Evolution of inflammation in nonalcoholic fatty liver disease: the multiple parallel hits hypothesis, *Hepatology* 52 (2010) 1836–1846.
- [36] B.P. Vaughn, S.C. Robson, G. Burnstock, Pathological roles of purinergic signaling in the liver, *J. Hepatol.* 57 (2012) 916–920.
- [37] G. Baffy, Kupffer cells in non-alcoholic fatty liver disease: the emerging view, *J. Hepatol.* 51 (2009) 212–223.
- [38] E. Gonzales, B. Julien, V. Serriere-Lanneau, et al., ATP release after partial hepatectomy regulates liver regeneration in the rat, *J. Hepatol.* 52 (2010) 54–62.
- [39] S. Jiang, Y. Zhang, J.H. Zheng, et al., Potential hepatic stellate cell activation by extracellular ATP is dependent on P2X7R-mediated NLRP3 inflammasome activation, *Pharmacol. Res.* 117 (2017) 82–93.
- [40] M.N. Sathe, et al., Regulation of purinergic signaling in biliary epithelial cells by exocytosis of SLC17A9-dependent ATP-enriched vesicles, *J. Biol. Chem.* 286 (2011) 25363–25376.
- [41] H. Sakai, M. Tsukimoto, H. Harada, Y. Moriyama, S. Kojima, Autocrine regulation of macrophage activation via exocytosis of ATP and activation of P2Y11 receptor, *PLOS One* 8 (2013), e59778.
- [42] Y. Harada, Y. Kato, T. Miyaji, H. Omote, Y. Moriyama, M. Hiasa, Vesicular nucleotide transporter mediates ATP release and migration in neutrophils, *J. Biol. Chem.* 293 (2018) 3770–3779.
- [43] N. Hasuzawa, S. Moriyama, Y. Moriyama, M. Nomura, Physiopathological roles of vesicular nucleotide transporter (VNUT), an essential component for vesicular ATP release, *Biochim. Biophys. Acta Biomembr.* 2020 (1862), e183408.